EFDA–JET–CP(13)03/02

T. Püetterich, R. Dux, R. Neu, M. Bernert, M.N.A. Beurskens, V. Bobkov, S. Brezinsek, C. Challis, J.W. Coenen, I. Coffey, A. Czarnecka, C. Giroud, P. Jacquet, E. Joffrin, A. Kallenbach, M. Lehnen, E. Lerche, E. de la Luna, S. Marsen, G. Matthews, M.-L. Mayoral, R.M. McDermott, A. Meigs, J. Mlynar, M. Sertoli, G. van Rooij, the ASDEX Upgrade Team and JET EFDA contributors

Taming Tungsten in JET and ASDEX Upgrade

Taming Tungsten in JET and ASDEX Upgrade

T. Püetterich[1], R. Dux[1], R. Neu[1,2], M. Bernert[1], M.N.A. Beurskens[3], V. Bobkov[1], S. Brezinsek[4], C. Challis[3], J.W. Coenen[4], I. Coffey[5], A. Czarnecka[6], C. Giroud[3], P. Jacquet[3], E. Joffrin[7], A. Kallenbach[1], M. Lehnen[4], E. Lerche[8], E. de la Luna[9], S. Marsen[10], G. Matthews[3], M.-L. Mayoral[2,3], R.M. McDermott[1], A. Meigs[3], J. Mlynar[11], M. Sertoli[1], G. van Rooij[12], the ASDEX Upgrade Team and JET EFDA contributors*

JET-EFDA, Culham Science Centre, OX14 3DB, Abingdon, UK

[1]Max-Planck-Institut für Plasmaphysik, EURATOM Association, 85748 Garching, Germany
[2]EFDA CSU, Boltzmannstr. 2, 85748 Garching, Germany
[3]EURATOM-CCFE Fusion Association, Culham Science Centre, OX14 3DB, Abingdon, OXON, UK
[4]Institute of Energy- and Climate Research, Forschungszentrum Jülich, Association EURATOM-FZJ, Germany
[5]Queen's University Belfast, University Road, Belfast BT7 1NN, Northern Ireland, UK
[6]EURATOM Association, Inst Plasma Phys & Laser Microfus, PL-01497 Warsaw, Poland
[7]CEA, Assoc. EURATOM-CEA, IRFM, Cadarache 13108 Saint Paul Lez Durance, France
[8]Association EURATOM-Etat Belge, ERM-KMS, Brussels, Belgium
[9]EURATOM CIEMAT Association, Laboratory Nuclear Fusion, Madrid, Spain
[10]Max-Planck-Institut für Plasmaphysik, EURATOM Association, D-17491 Greifswald, Germany
[11]Association EURATOM-IPP.CR, Institute of Plasma Physics AS CR, 18200 Prague, Czech Republic
[12]DIFFER, Assoc. EURATOM-FOM, 3430BE Nieuwegein, Netherlands
** See annex of F. Romanelli et al, "Overview of JET Results", (24th IAEA Fusion Energy Conference, San Diego, USA (2012)).*

Preprint of Paper to be submitted for publication in Proceedings of the 40th EPS Conference on Plasma Physics, Espoo, Finland.
1st July 2013 – 5th July 2013

ABSTRACT

A short review of prior results on W-erosion, W-screening of the divertor and W-transport in the pedestal and the plasma core is given. The W-transport in the core plasma of JET is investigated experimentally by deriving the W-concentration profiles from modelling of the signals of the soft X-ray cameras. For the case of pure neutral beam heating W-accumulates in the core to W-concentrations of 10^{-3} in between the sawtooth crashes, which flatten the W-profile to a concentration of about $3 \cdot 10^{-5}$. When central ICRH heating is additionally applied the core Wconcentration decays in phases that exhibit a changed mode activity, while also the electron temperature increases and the density profile becomes less peaked. The immediate correlation between the change of MHD and the removal of W from the plasma core supports the theory that the change of the MHD activity is the underlying cause for the change of transport. Furthermore, two discharge scenarios from ASDEX Upgrade are investigated. In the first case the central W-radiation influences the core W-transport such that slowly increasing W-radiation leads to a steepening of the W-concentration profiles. In the second case two discharges are compared in which a small change of the heating trajectory leads to a change of the W-transport and a change of the sawtooth behaviour. It is speculated that the W-accumulation is the underlying reason for the irregular sawteeth, which in turn aids the W-accumulation.

1. INTRODUCTION

In ASDEX Upgrade (AUG) and JET tungsten (W) is used as a plasma facing material (cf. Ref. [1] for AUG and Ref.[2] for JET), because it will be used in ITER and it is a promising candidate material for a fusion reactor. While at AUG a stepwise approach to replacing the graphite wall tiles by W-coated ones was pursued from 1999-2007, the ITER-like wall (ILW) at JET consisting of Be (main chamber) and W (divertor) plasma facing components (PFCs) was implemented during one single vent in 2010/2011. A crucial task for plasma operation is the control of the W-concentration in the plasma core, as W may lead to unacceptable radiative cooling for concentrations above $\approx 10^{-4}$. As such it is important to know a good handle on the various mechanisms available to influence the control of the W-content of the core plasma. In the remainder of the introduction such mechanisms investigated at JET and AUG acting on W-erosion and W-transport are reviewed. In section 2 a detailed analysis of the W-transport in the core of JET discharges is presented, which emphasizes the importance of MHD for the central W-transport. In section 3 the correlation of W-transport and W-radiation is presented and discussed and finally, section 4 summarizes the results.

In the divertor of AUG, the erosion of W has been shown to be dominated by low-Z impurities such as carbon (C), boron (B) or oxygen (O)(e.g. Ref. [3]). Consistently, the W-erosion in JET with the ITER-like wall (JET-ILW) can be explained by sputtering by Be using the Be-fraction present in the main plasma (Ref. [4]), while C and O are of no importance in JET-ILW. After being reduced by a factor of 10-20 the resulting C-concentrations are about 0.05% (cf. Ref. [5]). An important parameter to influence the W-erosion is not only the mix of impurities and their concentrations in

the divertor plasma, but also the divertor temperature. As the impurity ions are accelerated in the plasma sheath, the electron temperature in the divertor determines sensitively the W- erosion, such that the inter-ELM erosion is closely related to the inter-ELM divertor temperature (cf. Ref. [3]). This effect can be exploited via radiative cooling of the edge and divertor plasma, e.g. by application of N-seeding, as was demonstrated in Ref. [4]. The erosion by ELMs strongly depends on their specific type with type-II and type-III ELMs producing much less W erosion than type I ELMs (see for example [6]), but also ELM-mitigation and supression techniques may be useful to reduce the W-erosion connected to type-I ELMs. It should be noted that eroded W-atoms may locally redeposit, if the gyration trajectory of the W-ion intersects the wall immediately after the ionization process. This so called prompt redeposition happens at a higher probability (cf. [7]) if the plasma in front of the plasma facing components is hot and dense like the plasma that is transported to the wall during an ELM.

A fundamental difference between JET-ILW and ASDEX Upgrade is the poloidal distribution of W-sources. JET-ILW features W-PFCs predominantly in the divertor, while at AUG, the outer limiters in the main chamber have been identified as the W-source with the largest impact on the W-concentration of the confined plasma (cf. Ref. [3]). This can be clearly shown, as the variations of the measured W-erosion flux from these limiters during a plasma position scan correlate with the evolution of the W-concentration. The W-fluxes from other sources were observed to either anticorrelate (inner heatshield, main chamber) or not change (divertor) at all. This is true even though the latter sources are larger by up to an order of magnitude. This relates to a different probability of eroded W-ions to be transported into the main chamber plasma. Investigations on the divertor retention of W (cf. [8]) in ASDEX Upgrade confirm the larger impact of the main chamber sources on the W-content of the main plasm as compared to the divertor sources. Only about 6% of the W eroded in the divertor managed to travel upstream into the scrape-off layer of the main chamber and only about 5% of these W-ions managed to enter the plasma. This means that for an eroded W-atom in the divertor, the probability is about 3×10^{-3} to end up in the main plasma. The investigated discharges were type-I ELMy H-modes at a plasma current of 1MA, a magnetic field of 2.5T, neutral beam heating of 5MW and a density of $7.5\times10^{19}\,m^{-3}$, which, in terms of retention, is not expected to yield an extreme case (neither high nor low). For JET, the divertor retention also was investigated in type-I ELMy H-modes, performed at a plasma current of 2MA, a magnetic field of 2.1T, neutral beam heating of 8-12MW and a density of about $6-7\times10^{19}\,m^{-3}$ (cf. Ref.[9]). The divertor erosion flux of W was compared to the W-content of the plasma. The ratio of the two is the W-confinement time which is the result of various transport effects, i.e. also including the divertor retention. The W-confinement time was then compared to the energy confinement time and was found to be about 150 to 400 times smaller, i.e. 0.6-2.5ms for an energy confinement time of 230-320ms (cf. Ref.[9]). At AUG this ratio was found to be roughly 300. Considering the mix of effects that contribute to this figure of merit, the results are very comparable.

The use of ion cyclotron resonance heating (ICRH) leads in both experiments to an increased

W-content of the confined plasma. At AUG detailed investigations on erosion locations demonstrated that the increase of the W-content of the plasma is dominated by W-erosion at the outboard limiters. The usage of ICRH leads to an increased sputtering yield resulting in an enhanced W-flux (cf. Ref. [10, 11]), which restricts the operational space for ICRH. For JET-ILW the increase of the W-source could not directly be localized, as the plasma wetted W-surfaces in the divertor do not exhibit an enhanced W-flux during ICRH. However, the activation of the W-source during limited plasmas not using the divertor and the suppression of the source after Be-evaporation in the main chamber suggest that additional W-sources in the main chamber are activated during ICRH. However, the suspected W-surfaces in the main chamber are behind protection limiters and negligible particle fluxes onto these are expected.

The impurity transport in the AUG H-mode pedestal was analyzed in Ref. [12] and it was found to be consistent with neoclassical transport. For a typical H-mode in AUG the convective transport for He, C, Ne and Ar was inward directed and scaled with the charge of the impurity. Also, the absolute values of the convective velocities and diffusion coefficients matched the neoclassical ones. Thus, steep density profiles for the impurities arose. For W, the density pedestal was modelled to feature a ratio of pedestal-top to separatrix density of around 100. This strong confinement of impurities requires a mechanism that regularly releases impurities, such as edge localized modes (ELMs). In Ref. [7, 12], the effect of ELMs was modelled for a series of discharges. The model describes the W-flushing by ELMS at the pedestal, while at the same time it takes into account that ELMs cause a considerable, additional W-source at the first wall. The net effect of a higher ELM-frequency was modelled to be always reducing the W-content of the main plasma. Thus, the effect of ELM-flushing is always predicted to outbalance the effect of the additional W-source due to ELMs. Experiments at JET have been performed using vertical kicks of the plasma to trigger ELMs. Plasmas with higher kick frequencies and therefore higher ELM-frequencies, are observed to be more stable [13] even at reduced gas fueling.

In the plasma core the effect of impurity accumulation is a well-known effect observed already in the limiter tokamaks PLT and ORMAK which were both operated with high-Z limiters (cf. Ref. [14, 15]). At ASDEX Upgrade and JET the operation with W PFCs is possible since the divertor concept helps to drastically reduce the W-content of the plasma [16]. However, core localized impurity accumulation is still observed in discharges where core neoclassical transport dominates the impurity transport in the plasma core [17]. This happens naturally, because the profiles of density and temperature have only small gradients in the plasma core. As turbulent transport requires a threshold in the gradients of the kinetic profiles there is always a small region in the core where neoclassical transport may be important, as has been shown for Ne, Ar, Kr and Xe in Ref. [18]. Similar to the edge pedestal, neoclassical transport in the core may lead to steep impurity gradients that cause strong local radiative cooling. The easiest way of preventing impurity accumulation has been shown to be central heating by electron cyclotron resonance heating (ECRH), ICRH or neutral beam heating [19]. The effectiveness of this approach has been attributed to an increased turbulence

level, rendering the neoclassical transport less important. The analyses of impurity transport (Si, Ar and Ni) for cases with central heating compared to cases without central heating in AUG [19, 20] and JET [21, 22] give larger diffusion coefficients and a reduction or even reversal of the convective velocity (cf. Ref.[19, 20]). In the next section a recently developed diagnostic method [9], which provides W-concentration profiles by modelling the soft X-ray emissions, is exploited in order to investigate further the transport of W in the core plasma of JET-ILW.

2. CORE TRANSPORT OF TUNGSTEN INVESTIGATED IN JET

The soft X-ray cameras at JET-ILW are used to derive the profiles of W-concentration and poloidal asymmetries due to centrifugal forces. The details of the diagnostics are described in [9]. The basic assumption that allows the determination of the W-concentration is that the low-Z impurities give rise to bremstrahlung, while the only other radiator is W, i.e. the radiation from Ni is negligible. The rotation velocity as derived from the poloidal in-out asymmetry provides a consistency check of that assumption. For the same rotation velocity the in-out asymmetry for W is larger than for a Ni. For the measured asymmetries the derived rotation velocities for W match those measured by charge exchange recombination spectroscopy, while those derived for the assumption that Ni is the main radiator would be about a factor of two too large. Generally, this observations holds in agreement to the spectroscopic observation that Ni contributes only a minor fraction < 10% even for plasmas with the highest Ni concentrations.

Two discharges with a plasma current of 2MA performed at a magnetic field of 2.7T are compared in the following. The first discharge (Pulse No: 83597) features ≈16MW of neutral beam injection (NBI) at a central density of about 7×10^{19} m^{-3}. The second, Pulse No: 83603, is heated with 14.5MW of NBI and an additional 3.5MW of central ICRH. The central density is about 6.5×10^{19} m^{-3}. The slight difference in density appears even though the deuterium gas fueling is equal for both discharges, i.e. 10^{22}D/s.

In Fig.1(a) and (b) the W-concentrations at r/a = 0.0,0.3 and 0.45 are depicted for both pulses. For Pulse No: 83597 (pure NBI), the core W-concentration at r/a = 0.0 shows large excursions compared to the values at r/a = 0.3 and 0.45. At these outer radii, the only excursion is provided by a W-event at about 15.5s, which increases the W-concentration from about 5×10^{-5} to 10^{-4}. The centralW-concentration varies between these values and about 10^{-3}. In Fig.1(c) and (d) the electron temperature measurements from electron cyclotron emission (ECE) channels close to the magnetic axis and close to the sawtooth inversion radius are presented. Using these signals as indicators of the sawtooth crashes a qualitative difference between the two discharges becomes apparent. For Pulse No: 83597 (pure NBI), the excursions of the W-concentration are aligned to the sawtooth crashes such that the sawtooth crash results in a flat W-profile, while in the phases between the sawtooth crashes theW-concentration rises constantly. For Pulse No: 83603 (NBI+ICRH), theW-concentration at r/a = 0.3 and r/a = 0.45 are slightly higher than in Pulse No: 83597 consistent with the increase of the radiated power from the main plasma as compared to Pulse No: 83597. In Pulse

No: 83603, the increasing and decreasing phases of the central W-concentrations (at r/a = 0.0) are not governed by the sawtooth cycle only. After a sawtooth crash, the W-concentration profile is flat, however, there are phases with decreasing W-concentration in between the sawteeth crashes. The interpretation of that observation is quite challenging and an attempt will be presented in the following. As an additional observation, the MHD behaviour as shown in Fig.1(e) and (f) seems to be quite different for the two pulses. For Pulse No: 83597 (pure NBI), a regular (1:1) mode is active during the the sawteeth cycle, while only a few perturbations of that mode activity are visible (cf. gray, transparent areas in Fig.1(a),(c) and (e)), e.g. one at 16.12 s. However, most of these special phases appear right after the sawtooth crash were density and temperature gradients are reduced, which could be the underlying reason for both, the changed transport and the changed mode activity: Right after the sawtooth crashes the mode activity is weaker and the inward transport of W pauses for about 50 to 100ms. For Pulse No: 83603 (NBI+ICRH), these phases also appear after the sawteeth crashes (cf. gray, transparent areas in Fig.1(b), (d) and (f)). Apart from these, more perturbations of the MHD activity (e.g. fishbones or jumps of the frequency of the (1:1) mode) show up regularly during the sawtooth cycle (cf. green, transparent areas in Fig.1(b), (d) and (f)) and correlate with the phases in which the W-concentration in the core decreases. Simultaneously, these phases also exhibit higher electron temperatures, which could also be a cause of changed transport. In the following we address these three questions:

- What drives the increase of the W-concentration after a sawtooth crash in Pulse No: 83597?
- Is the increased temperature for the ICRH case causing a neoclassical outward pinch?
- Is the change in MHD activity responsible for the removal of W from the plasma core?

In order to evaluate the neoclassical W-transport a close look at the ion density and temperature profiles is necessary. The gradients of the background ions (deuterium) lead to an inward convection, while the gradients in ion temperature lead to an outward convection. The electron density is used in the following to estimate the ion density. In Fig.2 the electron density profiles for the Pulse No's: 83597 and 83603 are depicted. For Pulse No: 83597 the density peaking in the core exhibits an evolution, such that it is fully developed only 50-100ms after the sawtooth crash. Thus, in order to estimate the neoclassical inward convection for W, the profiles from the second half of the sawtooth cycle are included in the fit. For Pulse No: 83603 no apparent evolution within the sawtooth cycle is observed, thus all measured density profiles are included. For the ion temperature in the plasma core no measurement is available. We therefore, use the electron temperature, which considering the high electron densities should be almost equal to the ion temperature. For Pulse No: 83603 strong localized core electron heating is provided by the ICRH, we therefore, consider the electron temperature as an upper limit for the ion temperature. In order to make this discussion for Pulse No: 83603 less complex, we use, for further considerations, only one temperature profile within the phase of the sawtooth cycle, i.e. the one featuring the highest central temperatures (≈6 keV) and thus the strongest neoclassical outward convection. The electron temperatures measurements

at the center and at the sawtooth inversion radius are presented in Fig.1 (c) and (d). The effect of impurities on the neoclassical transport coefficients is taken into account by NEOART and requires the input of impurity densities. In the following we assume constant impurity concentration profiles (1.5% cBe and 10^{-4} cW). Both values are in the right ball park according to the data from the visible Bremstrahlung (Be) and the soft X-ray cameras (W). Using the presented electron density profiles, the electron temperatures as measured by electron cyclotron emissions and the mentioned assumptions on impurity densities the neoclassical diffusion coefficients for W, as evaluated by NEOART, are around $0.015 m^2 s^{-1}$ for both cases (cf. Fig.2(e)and (f)). The profiles of the drift velocities for W are shown in Fig.2 (c) and (d). In both cases the most central transport is directed inward giving rise to accumulation, while at about r/a ≈0.15 the drift velocity reverses and is directed outward. The outward convection is only partly due to the temperature gradients, as a bump in the density profiles between r/a ≈0.25 and r/a ≈0.55 gives rise to flat (Pulse No: 83597) or slightly hollow (Pulse No: 83603) density profile at r/a ≈0.2. It is unclear if this bump is an artefact. For transport modelling, the neoclassical transport is combined with anomalous transport, which is in the present analysis assumed ad hoc.

The exact profile of the anomalous diffusion coefficient determines in which radial region the drift velocity has the biggest impact on the impurity profile. Under the assumption that a large diffusive transport is active only outside of r/a ≈0.20 (cf. depicted diffusion coefficients in Fig.2(e) and (f)), the neoclassical transport coefficients may be used to model the change of W-concentrations at r/a = 0.0 during a sawtooth cycle. The level of the anomalous diffusion coefficients have been chosen such that approximately the impurity confinement time (a few 100ms) from experiment is reproduced and at the same time the core transport stays at the neoclassical level. The actual experiments do not allow to determine a full D and v profile outside of the sawtooth inversion radius. Indeed, the discussed increase of the W-concentrations in the plasma core of Pulse No: 83597 can be described (cf. Fig.3) with transport coefficients reasonably close to the depicted (cf. Fig.2(c) and (e)) transport coefficients. In Fig.3 the results of two simluations are presented; one using exactly the transport coefficients as shown in (cf. Fig.2(c) and (e)) and one using twice the presented inward convection. The measured W-concentrations suggest that the real transport features drift velocities close to the latter coefficients. Considering the uncertainties in the density profile measurements this agreement is interpreted as a consistency between neoclassical transport and the observed dynamics of the W-concentration. For Pulse No: 83603, the measurements cannot be described by the depicted transport coefficients, as especially the innermost part of the neoclassical transport r/a < 0.2 always produces a peaked profile in the core. Note that this direction of the neoclassical drift velocity is still inward even though the temperature profile featuring the highest temperatures during the sawtooth cycle are taken into account, such that the inward convection is even stronger for most time points of the sawtooth cycle. This suggests that a change of the diffusive transport or an additional outward convection must apply in Pulse No: 83603, which cannot be explained by neoclassical theory. This could result from a change of turbulence in the plasma core or due to changed MHD activity. The

fact, that the phases with decreasing W-concentrations correlate clearly and immediately with the change in MHD activity without time lag suggests that the MHD activity is the underlying reason for the change of the W-content, which in terms of transport coefficients may be identified as a larger anomalous diffusion coefficient or an outward drift velocity (e.g. [20]).

3. FEEDBACK-LOOP BETWEEN TRANSPORT AND RADIATION

Due to the fact that W may radiate strongly in the plasma core (cf. Ref. [23]), new issues for plasma operation arise. Most of these issues are caused by the fact that the core radiation can influence the W-transport in such a way that feedback-loops are formed, an occurrence that is not possible for low-Z impurities. In Ref. [16] a feedback cycle of core radiation and ELM frequency was already discussed, while here we address the influence of core radiation on core transport by looking at dedicated discharges.

Figure 4 shows time traces from an AUG discharge in which all parameters are kept as constant as possible from 3 to 6s. The only parameter that is varied is the deuterium gas puff, which is ramped down continuously (cf. Fig.4(b)). The applied heating power is 7.5MW of NBI and 600 kW of central ECRH (cf. Fig.4(a)). The radiated power including the divertor radiation changes from about 4MW to 4.5MW (cf. Fig.4(a)), which is consistent with the change of the mid-radius W-concentration from 1.5×10^{-5} to 3.0×10^{-5}. It should be noted that the electron temperatures (cf. Fig.4(c)) and densities (cf. Fig.4(d)) do not change within the scatter of the data. This is true for the individual chords of the interferometer, and thus also for their ratio. Also, the electron temperatures close to the plasma core ($r/a \approx 0.2$) do not change. Still, the change at the plasma edge, i.e. the gas puff, causes the W-content at mid-radius to slowly rise. Probably as a consequence the core transport also changes as can be seen by the increasing core W-concentration, which increases by a larger factor than the W- concentration at mid-radius (cf. Fig.4(e) and (f)). This effect becomes more enhanced and is well visible from 5s on. The change of the impurity density profile is matched by the bolometer signals, which reproduce a steepening of the radiation profile. The depicted radiation ratio attributes the excess signal of a central bolometer chord to a region in the plasma core that has a diameter of about 10cm. The interpretation of the observation is that due to the change in gas puff the edge source of W is increased which affects the radiation losses in the whole volume of the confined plasma. As a change in transport can only be explained by changed temperature or density profiles the transport may only be affected inside of $r/a = 0.2$, where we do not have a temperature measurement available. Alternatively, the transport is affected by changes of the kinetic profiles that are not visible within the scatter of the data. Note that the MHD activity in the core did not drastically change. Clearly, the increased core radiation has an impact on core transport, such that even more radiation is emitted in the plasma core. If the central ECRH was not applied this feedback-loop would be happening much faster as can be seen in comparable discharges without ECRH.

In Fig.5 (a) and (b) two discharges are depicted that are nearly identical until 0.8s. From 0.3s onward, neutral beam heating is used to aid the current ramp by increasing the electron temperature.

As a side effect, current diffusion into the plasma core is hindered and the q-profile stay just above or close to 1 in the vicinity of the magnetic axis. For Pulse No: 24923, the 2.5MW of beam heating are kept until 1s and is then reduced to 1.3MW (Fig. 5(a)) by using a beam with reduced voltage, which also penetrates less deeply into the core of the plasma. This leads to core localized radiation, as can be seen by comparing a central chord of the bolometers to an off-central chord. Also visible in the bolometer signals is the absence of sawteeth meaning that the core radiation is not regularly reduced. The radiative cooling in the core seems to prevent the sawteeth, possibly by reducing temperatures enough to change the shape of the electron temperature profile and thus of the conductivity profile, which may reverse the direction of current diffusion. As soon as the central ECRH is added, the central radiation drops. The overshoot of the bolometer measurement to negative values at 2.0s is a diagnostic artefact that appears after steep drops of radiation. As the details of the q-profile, which are important to judge the existence of the q=1 surface, are difficult to diagnose, a second discharge (Pulse No: 24925) is performed, in which a short gap in the heating at 0.8s is applied with the intention of increasing the current diffusion and thereby obtaining a $q = 1$ surface in the plasma core. While the stop of neutral beam heating at 0.8s in Pulse No: 24925 has also an effect on radiation and a slight effect on densities, regular sawteeth indeed develop at 1.05s, just after the beam with reduced voltage (about 1.1MW) is switched on. This delay of the sawteeth is consistent with typical current diffusion times and thus the onset of sawteeth is not related to the switching on of the beam. It may be discussed, whether a change of the q-profile is the important difference between the discharges, because there is no unambiguous measurement of the core q and other parameters such as density and radiation profile are also slightly different for the two discharges. However, a clear observation is that a small difference in the applied heating trajectory causes a bifurcation in the behaviour of impurity accumulation. Bifurcations are always connected to non-linear dependencies and here the non-linearity must be related to the developments in the plasma core - either connected to transport or to the q-profile development.

4. SUMMARY AND CONCLUSIONS

The core transport in type-I ELMy H-modes has been investigated for JET plasmas with a plasma current of 2MA, toroidal field of 2.7T, a fueling gas puff of 10^{22} m^{-3} and about 16MW/14.5MW of beam heating. One plasma with central ICRH has been compared to a plasma without central ICRH. The plasma without ICRH yields a strong increase of the W-concentration from about 3×10^{-5} up to 10^{-3} within $r/a = 0.3$ during a sawtooth cycle and the sawtooth crash results in an approximately flat W-concentration profile. Within the uncertainties this cycle can be understood by neoclassical transport coefficients. When adding central ICRH the W-content of the plasma at $r/a = 0.45$ and $r/a = 0.3$ increases to about 10^{-4} and the central excursions of the W-concentrations become smaller and become even negligible. Due to a slight change in electron density and a strong change of temperatures, the neoclassical transport towards the core is less strong, but the detailed behaviour is best explained by an increased diffusive transport or temporary outward convection.

Due to the immediate correlation between a change of transport and a change of MHD activity the underlying reason for the different transport is attributed to the mode activity rather than to effects from turbulent transport or neoclassical transport.

From ASDEX Upgrade two different cases are presented which shed light on feedback mechanisms between W-radiation and W-transport. In the first case, the heating, density and temperatures stay constant within the experimental uncertainties, while the fueling gas puff is slowly reduced. This causes a rise of the W-source at the edge which becomes visible through a rise of the W-concentration at mid radius. Simultaneously, the W-transport changes producing steeper W-concentration gradients. The underlying changes of temperature and density either take place inside of $r/a = 0.2$ or are not visible within the scatter of the experimental data. Clearly, a core transport effect is achieved by the change of the edge source, while the plasma outside of $r/a = 0.2$ is not noticeably affected.

In the second case, a pair of discharges is compared for which the core behaviour of W-transport is drastically different. The discharge which exhibits strong W-accumulation and nearly no sawteeth is heated continuously by neutral beams, startingalready at 0.3 s. The second discharge is also heated from 0.3s on by neutral beams, but then neutral beam heating is interrupted for 0.2 s resulting in a discharge without W- accumulation and regular sawteeth. One interpretation aims to explain the differences by the effects on the q-profile due to a stop of auxiliary heating, which accelerates current diffusion, and due to W-radiation in the core, which may change the shape of the electron temperature profile possibly reversing the direction of current diffusion. Both effects suggest that in the first case the central q is above 1 and stays above 1 preventing regular sawteeth as the q=1 surface is not present in the plasma.

In conclusion, numerous tools to control W-erosion, W-transport and thus the W- concentration are known and are continuously used at ASDEX Upgrade and successfully transfered to JET. As, however, the predictive capabilities for future plasmas are still limited the resulting implications for controlling W are uncertain; a small change in the density profile will translate into a strong effect for W-transport. The quantitative understanding of the transport effects are limited also for today's devices, e.g. for predicting the necessary mode activity to prevent W-accumulation in the core and the interaction between mode activity, turbulent transport and neoclassical transport. Possibly all issues due to W in the main plasma are strongly relaxed for large devices such as ITER, as a recent study [24] concerning the neoclassical W-transport at the edge pedestal of ITER predicts an outward convection. As shown here this has not only implications on radiative losses of the confined plasma, but also on the stability of W-transport in the plasma core.

ACKNOWLEDGEMENT

This work was supported by EURATOM and carried out within the framework of the European Fusion Development Agreement. The views and opinions expressed herein do not necessarily reflect those of the European Commission.

REFERENCES

[1]. R. Neu et al., Physica Scripta **T138**, 014038 (6pp) (2009).

[2]. G. F. Mathews et al., Journal of Nuclear Materials **438**, S2 (2013).

[3]. R. Dux et al., Journal of Nuclear Materials **390-391**, 858 (2009).

[4]. G. J. van Rooij et al., Journal of Nuclear Materials **438**, S42 (2013).

[5]. S. Brezinsek et al., Journal of Nuclear Materials **438**, S303 (2013).

[6]. R. Neu et al., Journal of Nuclear Materials **438**, S34 (2013).

[7]. R. Dux, A. Janzer, T. P¨utterich, and ASDEX Upgrade Team, Nuclear Fusion 51, 053002 (2011).

[8]. A. Geier et al., Plasma Physics and Controlled Fusion **44**, 2091 (2002).

[9]. T. Püetterich et al., Proc. of the 24rd IAEA Fusion Energy Conference, San Diego, USA (IAEA, Vienna, 2012), Vol. IAEA-CN-197, pp. TH/P2–21.

[10]. R. Dux et al., Journal of Nuclear Materials **337-339**, 852 (2005).

[11]. R. Dux et al., Journal of Nuclear Materials **363-365**, 112 (2007).

[12]. T. P¨utterich et al., Journal of Nuclear Materials **415**, S334 (2011).

[13]. E. de la Luna et al., Proc. of the 24rd IAEA Fusion Energy Conference, San Diego, USA (IAEA, Vienna, 2012), Vol. IAEA-CN-197, pp. TH/P2–21.

[14]. R. Isler, R. Neidigh, and R. Cowan, Physics Letters A **63**, 295 (1977).

[15]. E. Hinnov and M. Mattioli, Physics Letters A **66,** 109 (1978).

[16]. R. Neu et al., Nuclear Fusion **45**, 209 (2005).

[17]. R. Neu et al., Journal of Nuclear Materials **313–316**, 116 (2003).

[18]. R. Dux et al., Nuclear Fusion **39**, 1509 (1999).

[19]. R. Dux et al., Plasma Physics and Controlled Fusion **45**, 1815 (2003).

[20]. M. Sertoli et al., Plasma Physics and Controlled Fusion **53**, 035024 (2011).

[21]. M. Puiatti et al., Physics of Plasmas **13**, (2006).

[22]. M. Valisa et al., Nuclear Fusion **51**, (2011).

[23]. T. Püetterich et al., Nuclear Fusion **50**, 025012 (9pp) (2010).

[24]. R. Dux et al., this conference, P4.143.

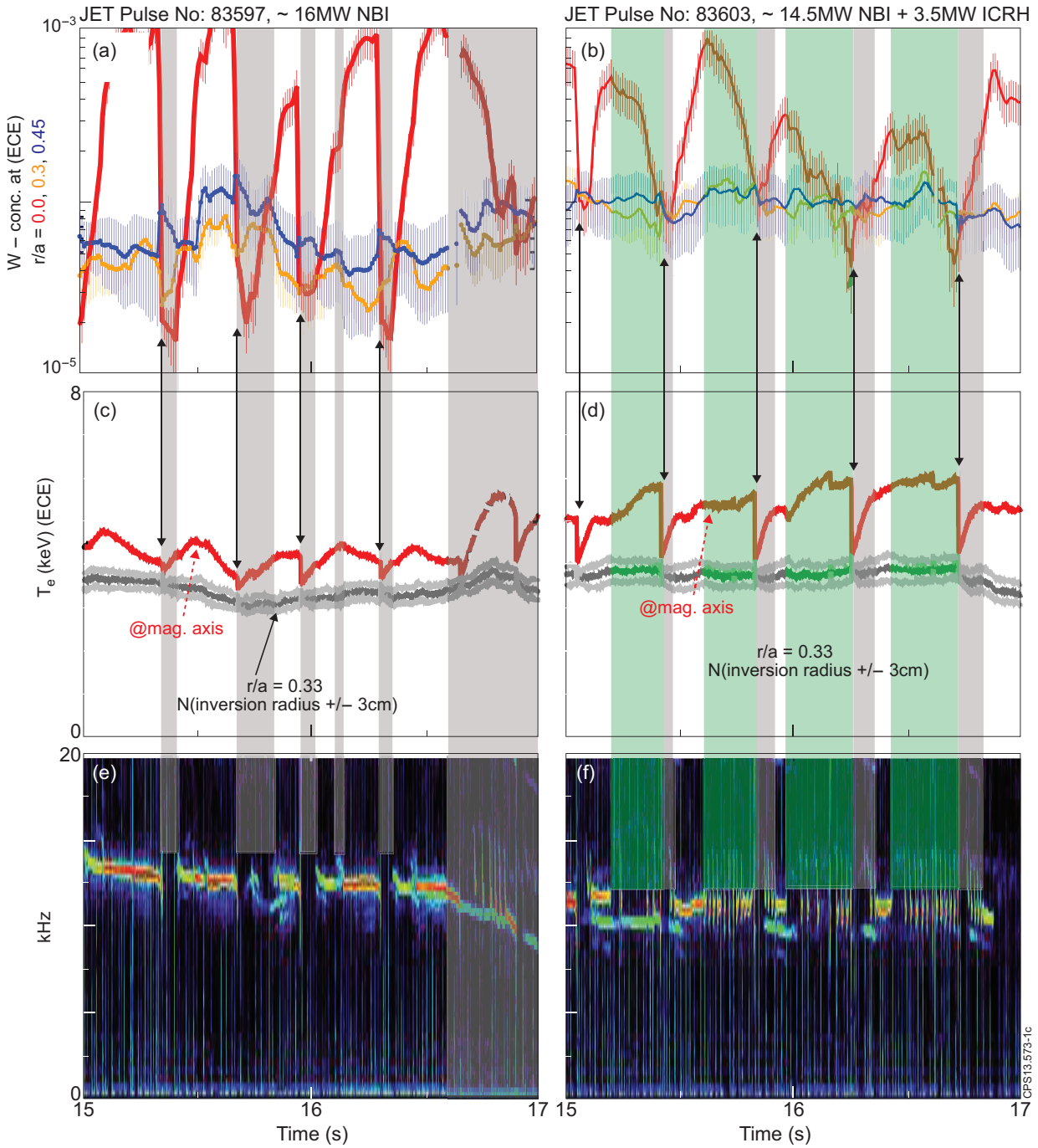

Figure 1: (a) and (b) Evolution of the W-concentrations at three radii for Pulse No's: 83597 and 83603; (c) and (d) Electron temperatures close to the magnetic axis and close to the sawtooth inversion radius for Pulse No's: 83597 and 83603; (e) and (f) Spectrogram of a magnetic coil located at the outer midplane for Pulse No's: 83597 and 83603.

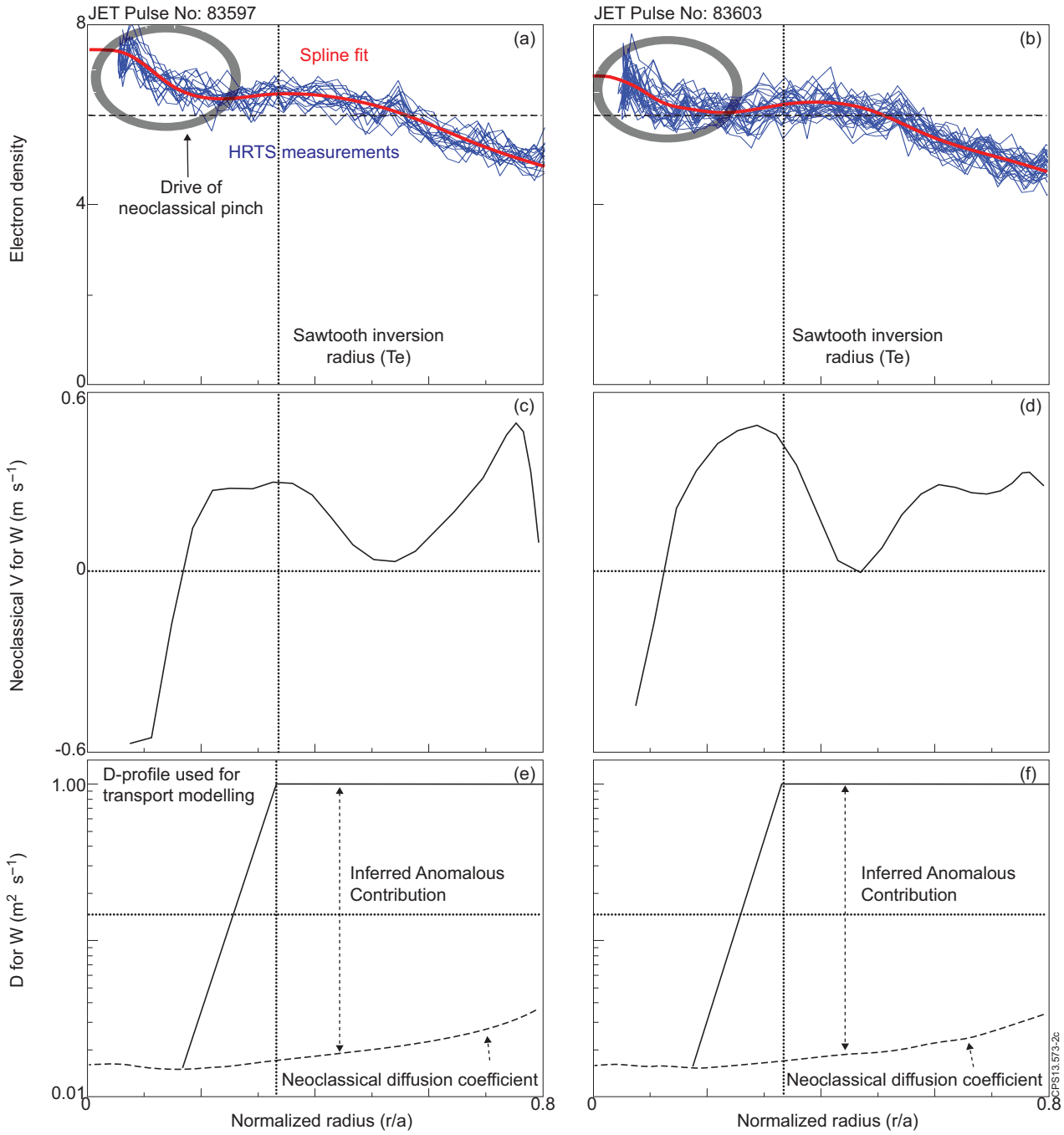

Figure 2: (a) Density profiles as measured by HRTS during the 2nd half of the sawtooth cycles in Pulse No: 83597 - data (blue), spline fit (red); (b) All density profiles as measured by HRTS during the time interval 15.0 to 16.5s in Pulse No: 83603 - data (blue), spline fit (red); (c) Drift Velocity for W as derived from NEOART using ne-profiles of part (a) and $T_i = T_e$ at the corresponding time points; (d) Drift Velocity for W as derived from NEOART using ne-profiles of part (b) and $T_i = T_e$ at the end of the sawtooth cycles; (e) W-Diffusion coefficient D as used in the transport modelling and neoclassical D as derived from NEOART using ne-profiles of part (a) and $T_i = T_e$ at the corresponding time points; (f) W-Diffusion coefficient D as used in the transport modelling and neoclassical D as derived from NEOART using ne-profiles of part (a) and $T_i = T_e$ at the corresponding time points.

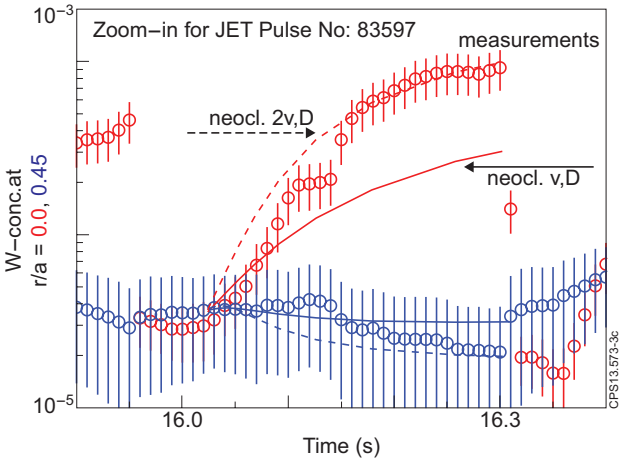

Figure 3: Zoom-in to one sawtooth cycle in Pulse No: 83597; The measured W-concentrations (symbols) at r/a = 0.0 (red) and r/a = 0.3 (blue) are compared to modelled ones using vneo and Dneo from neoclassical theory (solid lines) and using the $v = 2 \cdot v_{neo}$ *and* $D = D_{neo}$.

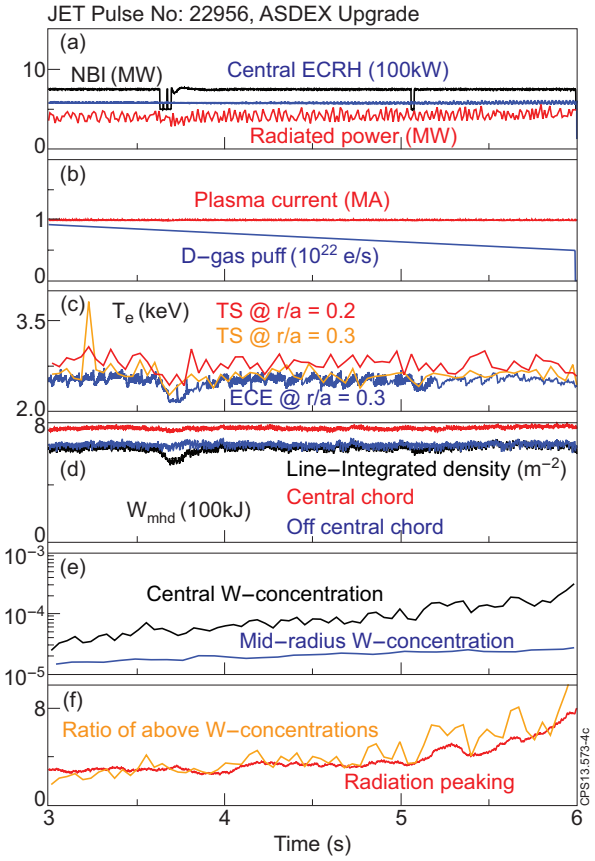

Figure 4: Time traces for Pulse No: 22956 in ASDEX Upgrade. (a) Power from neutral beam injection (NBI), central electron cyclotron resonance heating (ECRH) and radiated power; (b) plasma current and deuterium gas puff for fueling; (c) Electron temperatures from Thomson scattering (TS) and electron cyclotron emission (ECE); (d) Plasma stored energy (black) and line-integrated densities as measured by the DCN interferometer on a central (red) and off-central (blue) chord; (e) W-concentrations derived from spectroscopy corresponding to ion stages at mid radius and in the plasma core; (f) ratio of the above W-concentrations and ratio of the radiation density in the plasma core over bulk radiation density derived from bolometer chords assuming that accumulation occurs in a central region with a diameter of about 10cm.

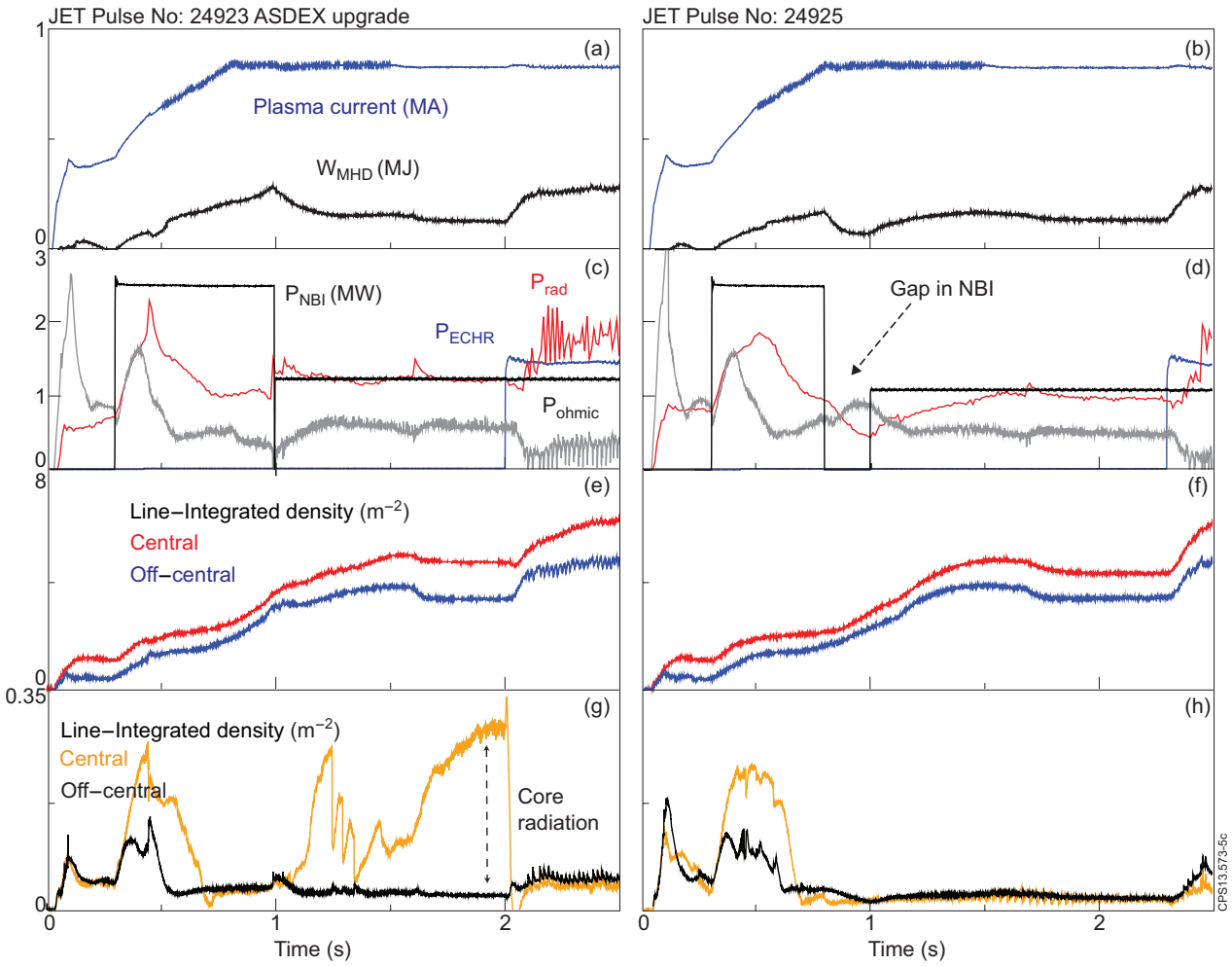

Figure 5: (a) Traces of the discussed quantities of Pulse No's: 24923 and (b)24925 in ASDEX Upgrade.